New Phytologist

Research

Plant hydraulics improves and topography mediates prediction of aspen mortality in southwestern USA

Xiaonan Tai[1], D. Scott Mackay[1], William R. L. Anderegg[2,3], John S. Sperry[3] and Paul D. Brooks[4]

[1]Department of Geography, University at Buffalo, 105 Wilkeson Quadrangle, Buffalo, NY 14261, USA; [2]Department of Ecology and Evolutionary Biology, Princeton University, Guyot Hall, Princeton, NJ 08544, USA; [3]Department of Biology, University of Utah, Salt Lake City, UT 84112, USA; [4]Department of Geology & Geophysics, University of Utah, Salt Lake City, UT 84112, USA

Author for correspondence:
Xiaonan Tai
Tel: +1 716 645 0495
Email: xiaonant@buffalo.edu

Received: *12 March 2016*
Accepted: *10 June 2016*

New Phytologist (2017) **213:** 113–127
doi: 10.1111/nph.14098

Key words: drought, forest mortality, plant hydraulics, spatial pattern, topographic convergence.

Summary

- Elevated forest mortality has been attributed to climate change-induced droughts, but prediction of spatial mortality patterns remains challenging. We evaluated whether introducing plant hydraulics and topographic convergence-induced soil moisture variation to land surface models (LSM) can help explain spatial patterns of mortality.
- A scheme predicting plant hydraulic safety loss from soil moisture was developed using field measurements and a plant physiology–hydraulics model, TREES. The scheme was upscaled to *Populus tremuloides* forests across Colorado, USA, using LSM-modeled and topography-mediated soil moisture, respectively. The spatial patterns of hydraulic safety loss were compared against aerial surveyed mortality.
- Incorporating hydraulic safety loss raised the explanatory power of mortality by 40% compared to LSM-modeled soil moisture. Topographic convergence was mostly influential in suppressing mortality in low and concave areas, explaining an additional 10% of the variations in mortality for those regions.
- Plant hydraulics integrated water stress along the soil–plant continuum and was more closely tied to plant physiological response to drought. In addition to the well-recognized topo-climate influence due to elevation and aspect, we found evidence that topographic convergence mediates tree mortality in certain parts of the landscape that are low and convergent, likely through influences on plant-available water.

Introduction

Rapid forest die-off can cause large-scale shifts in forest structure and composition, and consequently these events have strong feedbacks to climate (Allen & Breshears, 1998; Anderegg *et al.*, 2013b; Friend *et al.*, 2014). However, it remains challenging to predict the spatial–temporal pattern of forest mortality under novel climate conditions. This limitation has been attributed to the oversimplified and poorly constrained representation of mortality mechanisms in current models (Allen *et al.*, 2010; Fisher *et al.*, 2010; McDowell *et al.*, 2011; Anderegg *et al.*, 2015). Current Dynamic Global Vegetation Models (DGVMs) rely on logical but untested rules to represent mortality (McDowell *et al.*, 2011) and their underlying land surface models (LSMs) consider the soil–plant–atmosphere continuum as a one-dimensional column ignoring the spatial interaction (Fisher *et al.*, 2010). In this study, we identify two processes that are currently missing in models and attempt to evaluate whether incorporating them in models could improve the prediction of plants' response to drought.

First, there is a lack of physiological mechanisms to simulate tree mortality in regional-scale vegetation models (Allen *et al.*, 2010; Powell *et al.*, 2013). Most models can capture the reduced water available for plants during drought; however, large degrees of uncertainty exist among model predictions of elevated forest mortality (McDowell *et al.*, 2011; Powell *et al.*, 2013; Anderegg *et al.*, 2015). Decreases in soil water do not necessarily translate into comparable stress levels inside plants, such as hydraulic cavitation, stomatal closure and reduced photosynthesis. For instance, the same species growing on different soils have been shown to experience different levels of stress (Cobb *et al.*, 1997; Sperry & Hacke, 2002; Hogg *et al.*, 2008), and different species at the same site might have different vulnerability to cavitation (Breshears *et al.*, 2008; McDowell *et al.*, 2008). Consequently, there is a need for more physiologically realistic simulation of plant stress to explain mortality.

Growing evidence suggests that hydraulic dysfunction during drought is mechanistically related to tree mortality and predisposes trees to mortality (Anderegg *et al.*, 2012; Hartmann *et al.*, 2015). The impairment of vascular tissue is also interrelated with carbon starvation and/or biotic agent attacks (McDowell *et al.*, 2011, 2013; Gaylord *et al.*, 2013). Hydraulic safety, defined as the difference between a plant's maximum transpiration potential (E_{crit}) and the actual transpiration (E_c), has been

used to represent the level of plant vascular impairment (McDowell *et al.*, 2008). Hydraulic safety diminishes as drought progresses, and in theory, hydraulic failure could occur somewhere along the water transport pathway when the hydraulic safety drops to zero (Hacke *et al.*, 2000; McDowell *et al.*, 2008). Although climatic water deficit terms can capture reductions in plant-available soil water, hydraulic safety integrates the hydraulic response of the whole soil–plant–atmosphere continuum and is related more mechanistically to plant hydraulic dysfunction during drought (Fig. 1).

Second, studies typically account for spatial heterogeneity of tree mortality using either direct climatic variables or moisture indices derived from climatic variables (Rehfeldt *et al.*, 2009; Anderegg *et al.*, 2013a; Williams *et al.*, 2013; Worrall *et al.*, 2013). However, the role of topography in creating variations of micro-site condition within the same climate is considered insufficiently. Topography causes variations in both the energy and water input to forest systems, especially in complex terrains (Adams *et al.*, 2014). Elevation is often used as a surrogate for making spatial adjustments of temperature and precipitation, and hillslope aspect is used for quantifying radiation load (Körner, 2007; Rinehart *et al.*, 2008). Elevated mortality at low elevations and on sunward facing hillslopes is widely seen (Allen & Breshears, 1998; Frey *et al.*, 2004; Worrall *et al.*, 2008; Kaiser *et al.*, 2013). We complement those relatively well-known topographic effects in mediating climate extremes on mortality and focus on evaluating the role of topographic convergence.

Topography-driven convergence reorganizes the water balance driven by climate, creating persistently wetter valleys and drier ridges (Fig. 1). Its influence on the spatial structure of soil moisture is recognized to be prevalent from local to global scales (McDonnell *et al.*, 2007; Brooks *et al.*, 2011; Thompson *et al.*, 2011; Voepel *et al.*, 2011; Fan, 2015; Zapata-Rios *et al.*, 2015). Various hydroclimatic processes could be responsible for the co-evolution of soil moisture with topography. One frequently attributed process is the subsidy of groundwater (Fig. 1) (Clark *et al.*, 2015; Fan, 2015). As groundwater moves laterally from topographic divergent (e.g. convex ridges and divides) to topographic convergent (e.g. concave valleys and topographic hollows) areas (Dingman, 1994), it raises the water table towards the surface locally and thus supplies additional water to the root zone through capillary lift or hydraulic redistribution (Dawson, 1993; Liu *et al.*, 2006). Greater exposure to radiation and wind at ridges could also cause ridges to be drier compared to valley locations (Adams *et al.*, 2014). In addition, snow accumulation is correlated with surface convergence with thicker snowpack in concave areas, resulting in pockets of relatively higher soil water (Winstral & Marks, 2002). But the effects of topographic convergence on the spatial variations of soil moisture are often neglected in current mainstream LSMs (Nijssen *et al.*, 2001; Clark *et al.*, 2015; Fan, 2015). Given the critical role of soil moisture on plant development, incorporating this variability of soil moisture may improve predictions of drought-induced mortality compared to only considering the soil–plant–atmosphere column.

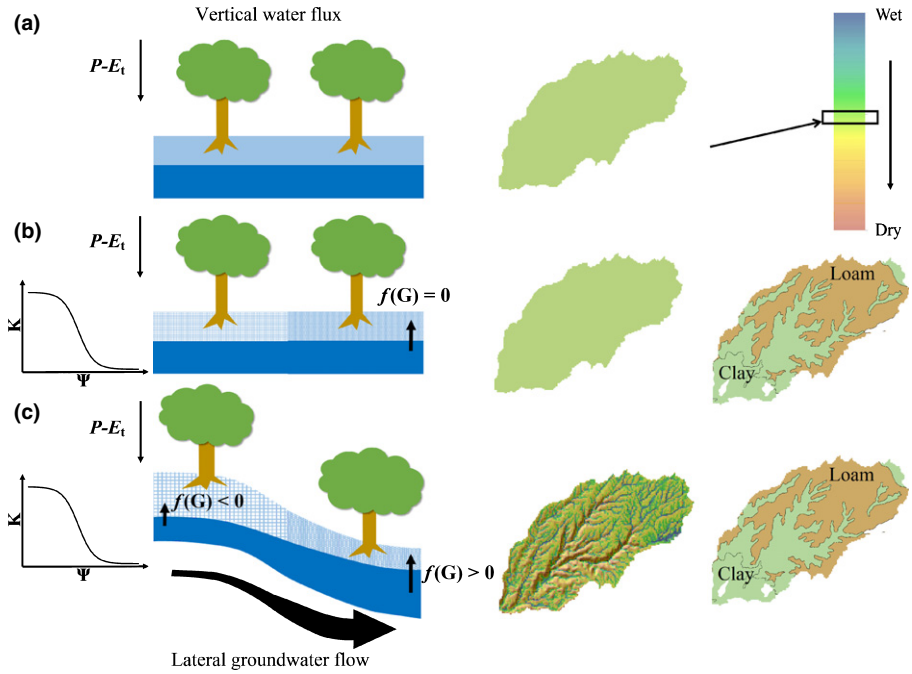

Fig. 1 (a) Plant water stress during drought is represented by soil water content solely accounting for the vertical water flux, which assumes homogeneous soil moisture within a simulation unit irrespective of topographic variations. *P* is precipitation and E_t is evapotranspiration. (b) Plant water stress is represented by hydraulic safety, which considers the response of the whole soil–plant–atmospheric continuum to drought. Hydraulic safety is derived by introducing plant hydraulic conductance (*K*) as a function of xylem water potential (Ψ). See Sperry *et al.* (1998) for details. (c) Lateral groundwater moves from divergent to convergent areas and causes variations in local groundwater table depth and thus reorganization of the soil moisture following topography. Color bar, the level of soil moisture wetness; *f*(*G*), subsidy of groundwater to root zone water storage; *f*(*G*) = 0, neutral area where there is no redistribution of soil moisture following topography; *f*(*G*) > 0, convergent areas that receive above average subsidy from groundwater; and *f*(*G*) < 0, divergent areas that receive below average subsidy from groundwater.

Tree mortality appears to be caused by a combination of stresses from climate, local habitat and biotic disturbances. Its incidence can lag behind the stressors by years or decades due to variations in individual genomic or phenotypic traits (Franklin *et al.*, 1987; Waring, 1987; Frey *et al.*, 2004; Suarez *et al.*, 2004; Anderegg *et al.*, 2013c). The mechanisms of mortality remain a focus of site-specific experiments and measurement campaigns (McDowell *et al.*, 2011), but spatial patterns of mortality observed from aerial photographs or remote sensing may also be used to gain insights on underlying mechanisms that are difficult to obtain in small-scale studies (Friend *et al.*, 2014; Anderegg *et al.*, 2015). Relying on the spatial observation of forest mortality at a regional scale, our goal is to provide a first-order explanation of regional mortality based on species hydraulic traits, general climatic conditions and micro-site topography. Specifically, we evaluate the following two hypotheses focusing on the improved representations of plant stress in the soil–plant–atmosphere column (one dimensional, hereafter 1D) and heterogeneity of plant stress associated with topography (three dimensional, hereafter 3D):

Hypothesis 1 – hydraulic safety better explains drought-induced mortality compared to soil water content estimated by models that do not account for the whole soil–plant–atmosphere continuum (Fig. 1a,b); and

Hypothesis 2 – hydraulic safety is a better correlate of mortality when incorporating the variability of soil water content induced by topography (3D) compared to soil water content driven by vertical water fluxes only (1D) (Fig. 1b,c).

Materials and Methods

Study area and data

We focused on trembling aspen (*Populus tremuloides* Michx., hereafter 'aspen') forests across Colorado, USA (Fig. 2). Aspen is one of the most widely distributed species and has experienced widespread die-off in the past 15 yr (in events called Sudden Aspen Decline, SAD) throughout western USA and southern Canada (Bartos, 2008; Hogg *et al.*, 2008; Rehfeldt *et al.*, 2009; Worrall *et al.*, 2013).

An overview of the methodology is shown in Fig. 3, including the validation dataset, input datasets and modeling steps. For validation we used a well-documented aerial survey of the SAD epidemic following the 2000–2003 severe drought across the complex terrain of the Colorado Rocky Mountains (Worrall *et al.*, 2008). Because the accuracy of aerial surveys has been found to be a few hundred meters (Huang & Anderegg, 2012; Anderegg *et al.*, 2015), our spatial analysis was performed using a 7.5 arc-second digital elevation model (DEM, *c.* 225 m on a side) (Danielson & Gesch, 2011) and STATSGO2 soil database (USDA, 2014) with comparable spatial resolution. The spatial information on soil water content was extracted from the NLDAS-2 project, which provided retrospective simulations from 1979 to present day in 1/8th degree grids (*c.* 13.5 km on a side) over the continental United States using four mainstream land surface models (LSMs) (Xia *et al.*, 2012b). All four LSMs simulated soil water content products that were found to be comparable and were validated against observations (Xia *et al.*, 2012a, b). We adopted the soil moisture product produced with the Variable Infiltration Capacity (VIC) model as it had previously been used to predict SAD (Anderegg et al., 2013a) and to study drought characteristics associated with climate change (Andreadis & Lettenmaier, 2006; Sheffield & Wood, 2008). We gathered the monthly mean soil moisture for growing season months – May, June, July, and August for 30 yr spanning from 1979 to 2008. Monthly soil moisture was used because it was found to be more reliable than short-term estimates and generally in equilibrium with meteorological forcing (Robock *et al.*, 2003; Sheffield *et al.*, 2004). In addition, ecophysiological measurements, including transpiration, leaf water potentials, soil moisture and

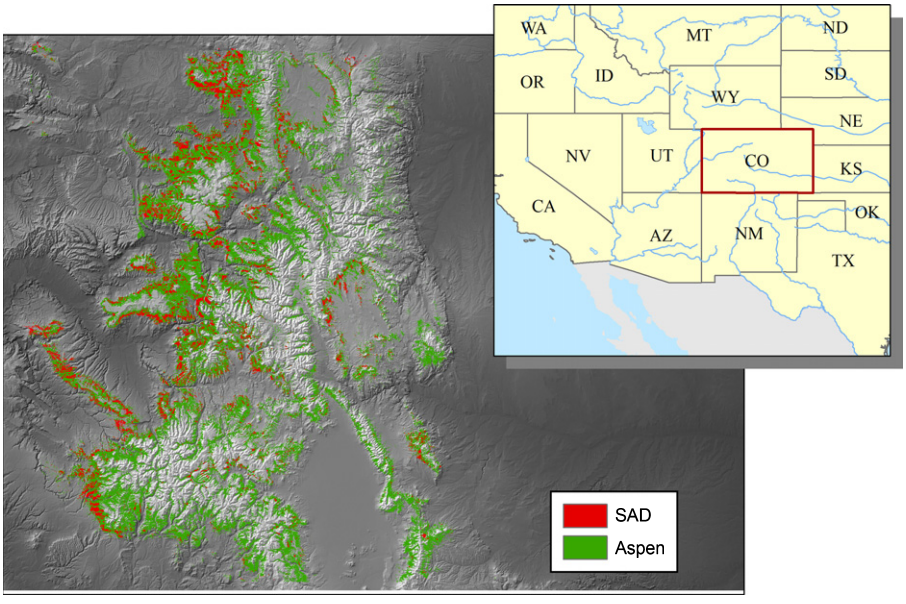

Fig. 2 Spatial extent of the study area (*c.* 27 000 km^2 aspen forest across Colorado, USA). SAD refers to the sudden aspen decline-affected (SAD) aspen.

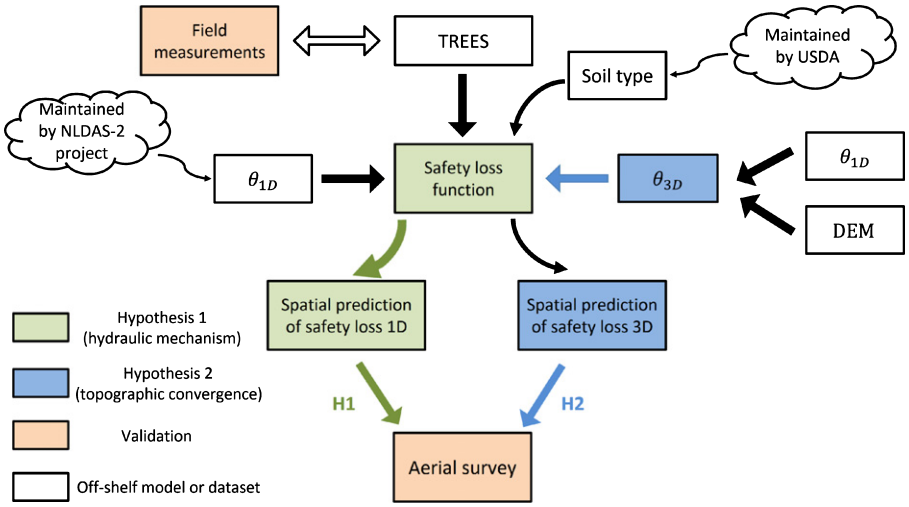

Fig. 3 Flowchart of hypothesis testing strategies. The hypotheses were tested using a combination of field physiological measurements, a plant physiologic model and existing products. We first developed a simple function to estimate hydraulic safety loss based on a plant physiological model that was parameterized and validated against field measurements. Then we extrapolated the function across space to generate the spatial estimation of 1D safety loss (green boxes). Hypothesis 1 was evaluated by comparing the explanation power of soil moisture vs 1D safety loss for mortality. To test Hypothesis 2 regarding topographic convergence, we developed an estimation of soil moisture, θ_{3D} and used it to derive 3D safety loss, approximating the effects of lateral convergence on soil moisture and consequently on plant safety loss. By comparing the explanatory power of 1D vs safety loss metrics for mortality, the importance of topographic convergent in accounting for mortality could be identified (blue boxes). DEM, digital elevation model; TREES, Terrestrial Regional Ecosystem Exchange Simulator

meteorological variables, were made at two aspen plots developing on loam soils, one visually healthy and one in the process of dying, during the 2012 growing season in San Juan National Forest, Colorado (Anderegg *et al.*, 2014).

Model of plant hydraulic safety

The hydraulic limit in the soil–plant–atmosphere continuum is determined by soil water content, soil hydraulic properties, transpiration and xylem vulnerability to cavitation (Sperry *et al.*, 1998; Bréda *et al.*, 2006). We used the Terrestrial Regional Ecosystem Exchange Simulator (TREES) (Mackay *et al.*, 2015) to compute hydraulic safety, as the difference between actual transpiration (E_c) and maximum transpiration potential (E_{crit}), because TREES integrates plant hydraulics, vulnerability to cavitation and canopy transpiration given half-hourly micrometeorological inputs. Descriptions of major processes and parameterizations of TREES can be found in Supporting Information Notes S1. Briefly, E_{crit} is derived using the steady-state hydraulic model described in Sperry *et al.* (1998), which explicitly solves the hydraulic gradient along the soil–plant continuum as well as the nonlinear decrease of hydraulic conductance associated with decreasing water potential (Sperry *et al.*, 1998; Mackay *et al.*, 2015). E_{crit} is the maximum potential value of E_c at which the corresponding hydraulic conductance approaches zero (Sperry *et al.*, 1998; Manzoni *et al.*, 2013). E_c is estimated in TREES by iteratively solving a series of equations including Fick's Law, Darcy's Law, Penman-Monteith, the Farquhar photosynthesis model and the detailed hydraulic model of Sperry *et al.* (1998), until convergence is reached so that it accounts for hydraulic limitation, atmospheric demand as well as photosynthesis (Mackay *et al.*, 2015).

Although it would be ideal to run TREES simulations across grids over the landscape, this is prohibited by limited biophysical and meteorological measurements available and the lack of a fully integrated model that accounted for both plant hydraulics and land surface processes. We therefore first assessed the ability of TREES to simulate *in situ* aspen stands (Anderegg *et al.*, 2014) by quantifying its predictions of transpiration, soil water content and leaf water potential compared to observations made in the field study site (Fig. 4). Then we relied on TREES to develop a simple yet biophysically constrained function to capture the first-order response of the soil–plant–atmosphere continuum to soil water availability.

Development of safety loss function for aspen

In order to develop a simple yet biophysically constrained function that can be used to predict aspen safety loss across the landscape, we used soil water potential as the predictive environmental variable because it is the driving force of the whole soil–plant–atmospheric hydraulic continuum (Sperry *et al.*, 1998; Manzoni *et al.*, 2013). The influences of other potential factors, such as vapor pressure deficit (VPD), were evaluated in a sensitivity analysis. Soil water potential depends on soil water content and hydraulic properties (hence soil texture). For southwestern US mountainous environments where a general decline in soil water is often observed throughout the summer months (Fig. S1) (Oglesby, 1991; Xia *et al.*, 2012b), early-season soil water content associated with snowmelt is critical for plant development (Fritts, 1974; Hanson & Weltzin, 2000; Bigler *et al.*, 2007; Williams *et al.*, 2013).

Consequently, we developed a dimensionless safety loss function for aspen, p, which related the average hydraulic safety,

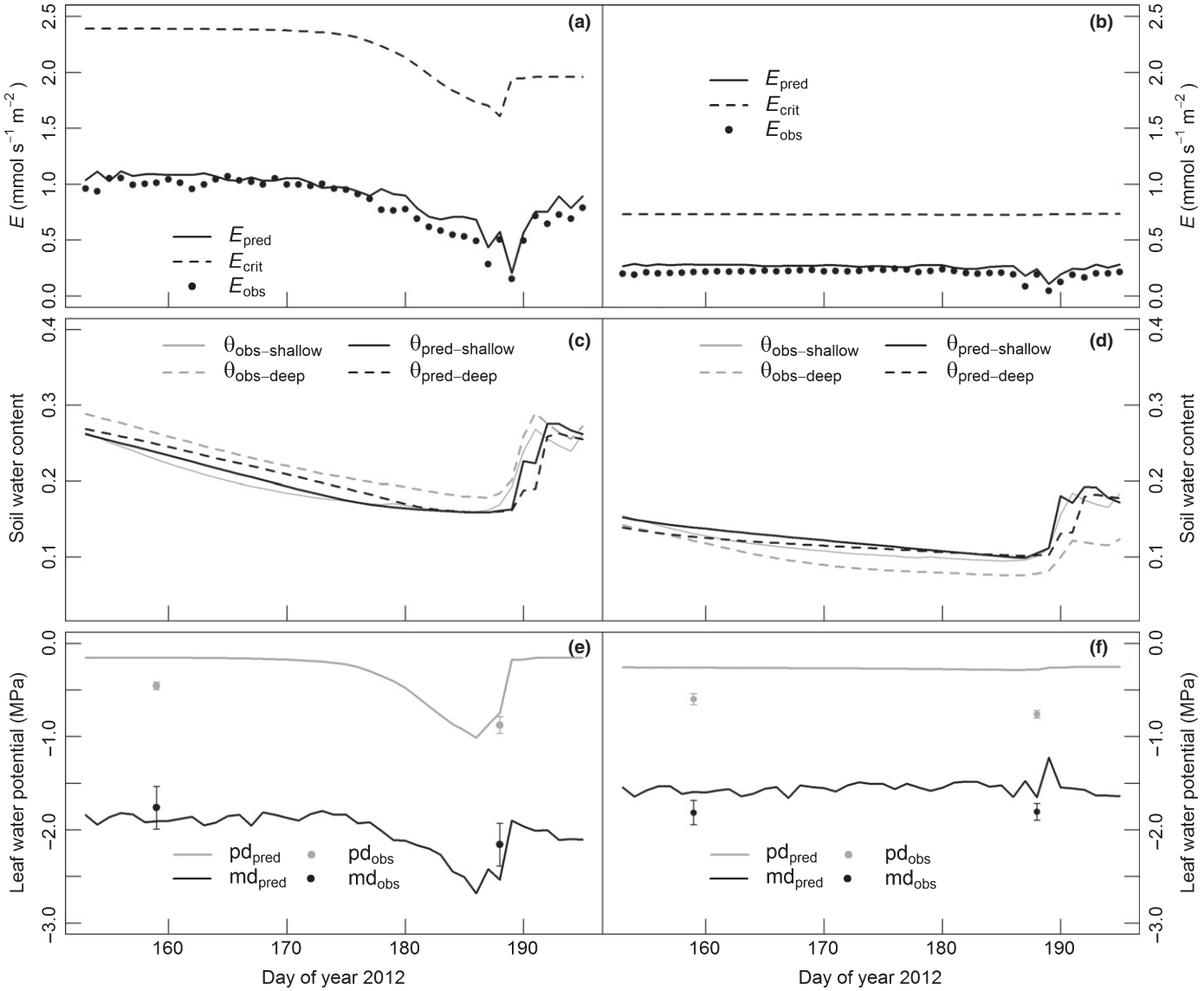

Fig. 4 Validation of Terrestrial Regional Ecosystem Exchange Simulator (TREES) showing predicted transpiration at midday (E_{pred}), predicted critical transpiration (E_{crit}), and measured transpiration (E_{obs}) (a, b); predicted shallow and deep soil moisture along with observation (c, d); and predicted leaf water potentials at predawn (pd) and midday (md) and measured leaf water potential ± SE (e, f) against date of year for a healthy stand (a, c, e) and a sudden aspen decline-affected (SAD) stand (b, d, f). R^2 for the healthy stand was 0.93 for transpiration, 0.89 for shallow soil moisture and 0.81 for deep soil moisture. R^2 for the sudden aspen death (SAD) stand was 0.76 for transpiration, 0.92 for shallow soil moisture, and 0.50 for deep soil moisture. Transpiration was measured using thermal dissipation sap flow sensors following the Granier method (Granier & Loustau, 1994). Soil water content at shallow (0–30 cm) and deep (30–60 cm) soil was measured using soil moisture probes (Campbell Scientific CS616). Leaf water potentials were measured with a Scholander-type pressure chamber (PMS Instruments, Corvalis, OR, USA). Predawn water potentials were measured at 03:00–05:00 h and midday potentials were measured at 12:00–14:00 h.

$\overline{(E_{crit} - E_c)}$, to soil texture and the initial soil water content of a general soil dry-down, as in Eqn 1.

$$p(\theta_{init}, \text{soil texture}) = 100\% * (1 - \frac{\overline{(E_{crit} - E_c)}}{(E_{crit} - E_c)_{max}}) \qquad \text{Eqn 1}$$

We simulated a rainless period of *c.* 5 wk long after snowmelt and before summer monsoon, because this is often the most stressful part of the year when plant growth is most active with high and relatively constant radiation in these forests (Anderegg *et al.*, 2013a, 2014, 2015). The average safety margin was used because it represented the level of hydraulic dysfunction over a sustained period encompassing a wide range of atmospheric conditions. The $(E_{crit} - E_c)_{max}$ term was the maximum value of $\overline{(E_{crit} - E_c)}$ associated with different initial soil water content and soil texture and was used to scale the safety loss metric over the range of 0–100.

We drove TREES using the meteorological records measured during the 5-wk rainless period from Day 153 to Day 187 of 2012. For a given soil texture, nine TREES simulations

were run with initial soil water contents (in volumetric units such as m^3 water m^{-3} soil) starting from 0.05 to 0.4 with 0.05 increments. For each initial soil water content, the average safety loss was derived from the corresponding half-hourly simulation of E_c and E_{crit} at midday (from 10:00 to 14:00 h) according to Eqn 1, and a sigmoid curve was fitted through the points. This was repeated for all soil texture types associated with aspen development in the region, resulting in a set of eight soil specific 'reference curves' that related p as a function of initial soil water content and soil texture (Fig. 5, curves of the same line type).

In order to evaluate the influence of other potential variables on these reference curves – namely, the particular time course of meteorological records used to drive TREES, the magnitude of VPD and the duration of soil dry-down – we performed a sensitivity analysis according to Table 1 in a factorial design, resulting in 27 sets of soil-type specific reference curves (Fig. S2). Meteorological forcing records were generated by randomly drawing daily samples with replacement from the measured record, and ± 20% change was induced to the measured VPD magnitudes. In addition to the 5-wk soil dry down, we also tested 6-wk and 7-wk dry down periods by randomly drawing daily samples with replacement from the measured meteorological record. Among the 27 sets of reference curves, three sets with the maximum, medium and minimum safety loss at a given soil water content (Fig. 5, curves of different line types) were selected to test the impact of reference curves on the spatial estimation of safety loss.

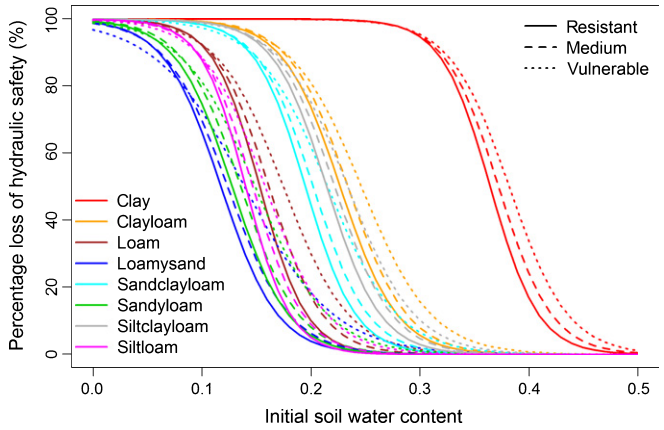

Fig. 5 Reference curves that estimated the percentage loss of safety (*y*-axis) as a function of initial soil water content (*x*-axis) and texture. Colors represent soil textures. For a given soil texture, simulations with various initial soil water content from 0.05 to 0.4 were carried and safety loss was derived according to Eqn 1. A sigmoid curve was fitted through safety loss and corresponding initial soil water content. The same procedure was repeated for the other seven soil types, yielding one set of reference curves (eight curves in total) estimating safety loss as a function of initial soil water content and soil type. Three sets of reference curves were presented here, representing the highest (dotted line), medium (dashed line) and lowest (solid line) safety loss at a given soil water content and texture, respectively. The R^2 for all fitted curves were > 0.9. These reference curves were used to relate 1D and 3D soil water content with safety loss across the landscape and to evaluate the influence of uncertainties in reference curve in the explanatory power of safety loss.

Table 1 Sensitivity analysis of reference curves to meteorological forcing time course, vapor pressure deficit (VPD) magnitude and rainless period duration

Factors considered	Procedure
Time course of meteorological forcing	Randomly distribute meteorological records used to drive the Terrestrial Regional Ecosystem Exchange Simulator (TREES) model; Repeated three times
VPD magnitude	Increase VPD by 20% Decrease VPD by 20% No change
Rainless period duration	5 wk 6 wk 7 wk

Spatial estimation of 1D and 3D soil water content

The VIC soil moisture product served as a proxy for climatically driven water availability for plants because it only accounted for the vertical water flux. We organized the computations on the basis of catchments with an average size equivalent to the size of a VIC grid cell. Catchments were delineated from the DEM. 1D soil water content driven by vertical water fluxes only 1D soil moisture, θ_{1D}, was computed as the catchment average soil water content weighted by the overlapping area between a VIC grid cell boundary and the catchment boundary.

Because the sub-grid heterogeneity of soil moisture induced by topographic convergence was missing in VIC and other NLDAS-2 products (Xia *et al.*, 2012a), we approximated it following a topographic framework (Famiglietti & Wood, 1994) based on the topography-soil index (λ_i) (Beven & Kirkby, 1979; Sivapalan *et al.*, 1987), defined as

$$\lambda_i = \log_e\left(\frac{aT_e}{T_i \tan\beta}\right) \quad \text{Eqn 2}$$

(i local grid cell index; T_e and T_i, catchment mean and local grid cell saturated transmissivity, respectively; tanβ, local grid cell slope; a, upslope contributing area per unit of contour width for the local grid cell). λ_i varies from relative high values in areas of topographic convergence, such as in hollows or along stream courses, to relatively low values where there is topographic divergence, such as at divides.

In spite of its recognized limitation, the λ_i index can be derived easily from readily available data and has been widely applied to represent the network-like topographic convergence of surface and subsurface water flow from local studies at scales of a few meters (Beven & Kirkby, 1979; Moore *et al.*, 1993; Adelman *et al.*, 2008) to regional studies at the kilometer scale (Chen & Kumar, 2001; Niu *et al.*, 2005). We calculated λ_i from the 225 m DEM and soil transmissivity, which is defined as the integration of soil hydraulic conductivity with depth through the soil profile, associated with the respective soil texture classes. Although λ_i cannot capture localized variations at scales of small forest stands,

it is a suitable surrogate for gross hillslope convergence and divergence at a macroscale (Wolock & Price, 1994; Quinn *et al.*, 1995) that is relevant for larger stands.

3D soil water content induced by topographic convergence, θ_{3D}, was derived by redistributing θ_{1D} within each catchment following a topographic framework (Famiglietti & Wood, 1994) as:

$$\delta_i = \lambda_i - \bar{\lambda} \quad \text{Eqn 3}$$

$$\theta_{3D,i} = \theta_{3D}(\theta_{1D}, \delta)_i = \theta_{1D,i} + m * \delta_i \quad \text{Eqn 4}$$

($\bar{\lambda}$, catchment average λ_i; δ_i, relative local topographic-soil index with respect to the catchment mean). The parameter m controlled the variance of local soil moisture to catchment average soil moisture through its similarity to the variance of local λ_i to catchment average $\bar{\lambda}$. A constant value of m was assumed, and a sensitivity analysis was performed using m from 0.001 to 0.010 with increments of 0.001. This formulation allowed representing the variation of soil water within a watershed as induced by lateral convergence (Fig. 1c). Convergent regions with positive δ were associated with higher than catchment average soil water, whereas divergent regions with negative δ had lower soil water compared to the catchment average.

Spatial estimation of 1D and 3D safety loss metrics

We obtained values of p for both the 30-yr average and drought years, and used the difference, Δp, as a safety loss metric to correlate mortality. Relative departure of water stress during drought from the stress levels experienced under the climatic normal incorporated the drought stress and potential plant adaptations to typically drier environments (Waring, 1987; Bréda *et al.*, 2006). 30-yr average was used to represent the climate normal because plant adaptation to hydrologic and climate conditions occurs over the period of a few decades (Mencuccini, 2003; Manzoni *et al.*, 2013). Because LSM simulated daily values were found to be less reliable (Sheffield *et al.*, 2004), we used the average soil water content of May and June spanning 2000–2003 to represent early-season soil water content during drought and the respective monthly average for the 1979–2008 period as climatology. We further included the months of July and August to compare which period of growing season was most useful to explain mortality.

For each location we used a soil map to determine which soil-type specific reference curve to use, and the values of soil water content determined the levels of safety loss for drought and climatology, respectively. We calculated the 1D safety loss, $\Delta p(\theta_{1D})$, as the difference of safety loss during drought relative to safety loss during the climate normal conditions. To test the importance of developing soil type-specific reference curves, we computed an alternative 1D safety loss, $\Delta p(\theta_{1D})$*, by assuming that the whole study area was covered with clay-loam soil, which was the dominant soil type in the region. The 3D safety loss, $\Delta p(\theta_{3D})$, was derived in a similar way to 1D safety loss by applying the safety loss function to spatial map of soil texture and θ_{3D}. To evaluate the first hypothesis (green boxes and arrows in Fig. 3), we compared the ability of 1D safety loss to predict aspen SAD to predictions made using soil water content only. To test the second hypothesis regarding topographic convergence (blue boxes and arrows in Fig. 3), we evaluated the ability of 3D and 1D safety loss to explain mortality.

Mortality along topographic gradients

We used Aerial Detection Surveys (ADS) obtained from the US Forest Service to quantify SAD-affected locations across gradients of elevation, aspect and topographic convergence. SAD-affected areas surveyed from 2008 to 2012 were merged regardless of the time detected, to capture the full spatial extent of SAD across Colorado. They were then converted to 30-m grid cells to correspond with a forest cover map derived from Landsat Thematic Mapper (Lowry *et al.*, 2007). Grid cells mapped as SAD but not classified as aspen on the forest cover map were excluded. Both SAD and aspen grid cells were aggregated to the same resolution of the DEM following the maximum aggregation rule (a coarse resolution cell was labeled as aspen/SAD as long as at least one of the fine resolution cell it contained was classified as aspen/SAD). In addition to the lateral gradient, hillslope aspect and elevation gradients were considered because they were found to be important topographic factors mediating plant mortality (Allen & Breshears, 1998; Worrall *et al.*, 2008; Huang & Anderegg, 2012). Hillslope aspect was derived following (Lammers & Band, 1990) and two categories were defined: 135°~315° and −45°~135° measured clockwise from north (referred to as S–W and N–E hereafter). The landscape was further discretized into elevation zones of 200-m intervals and then into groupings of equal δ intervals within each elevation zone within each aspect category. Because of the limited accuracy and precision of the ADS data, clumps of pixels (or effectively, aspen stands) sharing similar topographic characteristics (elevation, aspect and δ) were grouped together to reduce noise. This approach formed groups of stands with hydrologically similar conditions, although in some cases groups were not comprised of spatially contiguous stands. Mortality severity was calculated by dividing the count of SAD cells by the number of aspen cells falling within each group. The corresponding hydraulic safety loss metrics and soil water contents were computed from the average of all aspen pixels in each respective group. Spatial data processing was performed in GRASS (GRASS Development Team, 2014) and statistical analyses were carried out in R (R Core Team, 2015).

Results

Simulations of hydraulic safety loss using TREES

TREES simulations closely followed the observed sap flux, soil water content and leaf water potentials, for both the healthy and SAD aspen stands (Fig. 4). The predicted predawn and midday leaf water potentials were similar to measured values. In addition, it captured the differentiation of transpiration and, consequently,

hydraulic conductance between the healthy stand on relatively wet soils and the SAD stand on relatively dry soils.

The simulated reference curves demonstrated the nonlinear increase of safety loss to declining initial soil water content for all soil texture types (Fig. 5). At the same water content, plants exposed to coarse-textured soils experienced lower safety loss compared to plants growing on soils with higher clay content. The reference curves remained relatively stable with varying meteorological time course and magnitude of VPD, whereas the longer dry-down duration caused higher safety loss at the same initial soil water content (Fig. S2, different line types).

Observed topographic variations in mortality

The magnitude of mortality varied mainly along the elevational gradient, with high mortality in low elevations, regardless of topographic convergence/divergence and aspect category (Fig. 6). The peak of mortality severity occurred at a lower elevation than the peak of aspen abundance. In convergent ($\delta > 0$) and low-elevation regions, mortality became less severe as δ increased (Fig. 6a,c). By contrast, in divergent regions ($\delta < 0$; Fig. 6b,d), there was little response of mortality to changes in δ. The only exception was *c.* 10% of the total aspen covered areas in the low-elevation zones on S–W aspects, where mortality unexpectedly decreased as δ became more negative (or more divergent; Fig. 6d).

Hydraulic safety loss vs soil water content as correlates of drought-induced mortality

Hydraulic safety loss improved the fraction of explained variance from 24% by soil water content to 62% (Table 2).

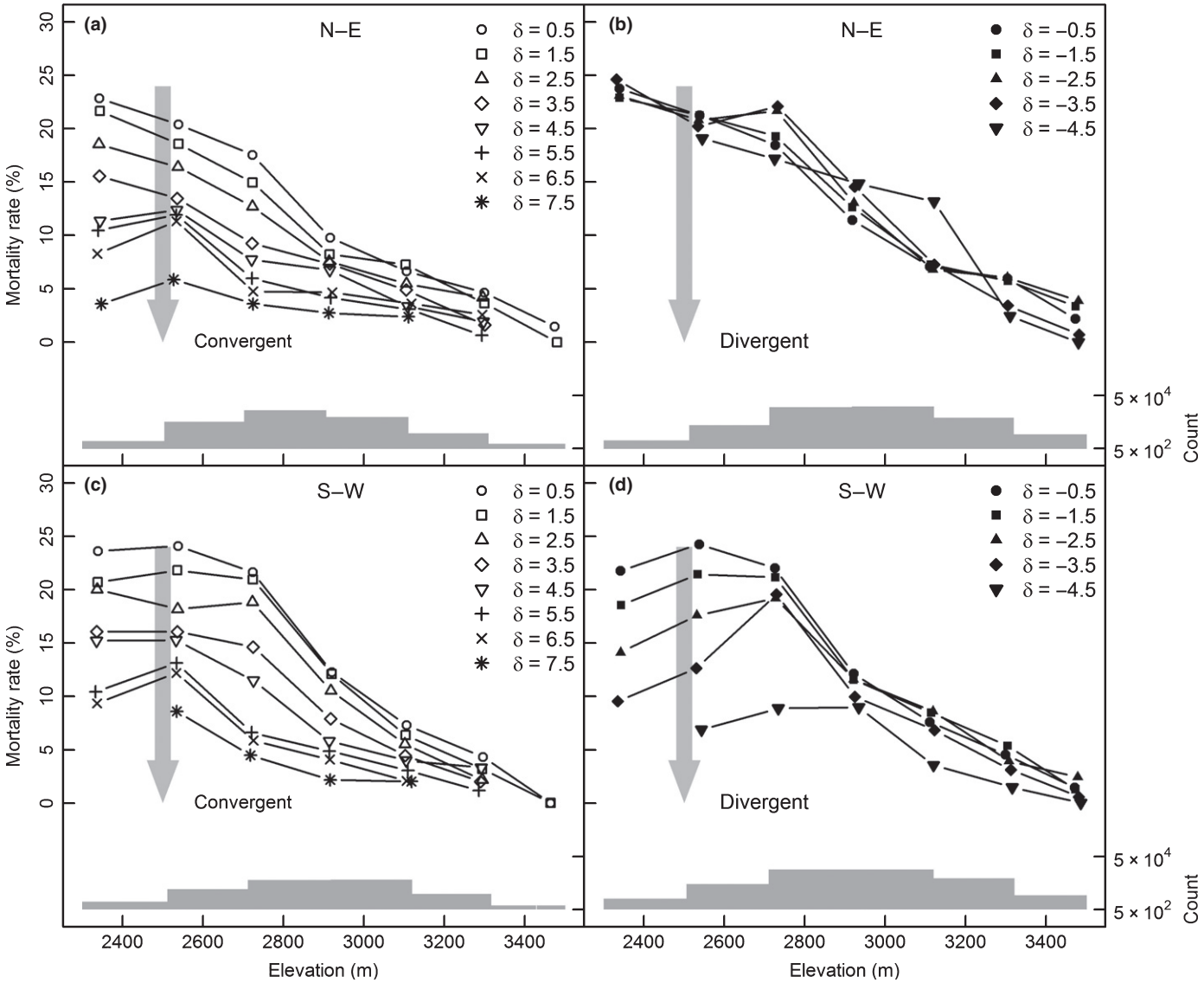

Fig. 6 Observed mortality along topographic gradients for convergent regions (a, c) and divergent regions (b, d). (a, b) Regions with N–E hillslope aspect; (c, d) regions with S–W hillslope facing aspect. Horizontal axis represents elevation zones with 200-m intervals and different symbols represent groups with different values of δ (a more positive value represents areas that are more convergent receiving more groundwater subsidy, whereas a more negative value represents more divergent areas with less subsidy). Also shown in the bottom are the counts of aspen pixels (*c.* 225 m per side) within each elevation zone.

Table 2 Summary of regression statistics between mortality severity and alternative models to explain drought-induced mortality across the whole landscape based on average 2000–2003 June soil moisture using 'medium' reference curves

Variable	Intercept	Slope	R^2	*P*-value
$\Delta\theta_{1D}$	−28.6	−17.69	0.24	< 0.01
$\Delta p(\theta_{1D})$	−6.6	2.36	0.62	< 0.01
$\Delta p(\theta_{1D})$*	−13.8	1.92	0.37	< 0.01

$\Delta p(\theta_{1D})$* denotes the 1D safety loss estimation assuming a single soil type of clay-loam without spatial information of soil type.

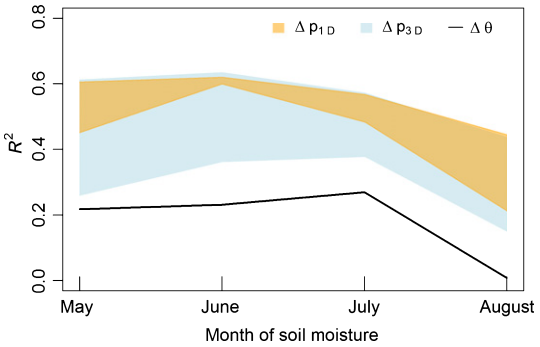

Fig. 7 Variance of aspen mortality explained by 1D safety loss using different reference curves (orange shaded region), 3D safety loss using different reference curves and values of m (light blue shaded region), and soil water content (solid line) by summer months.

Uncertainties in reference curve selection (associated with highest, medium or lowest safety loss for a given soil water content) had minimal impact on this general improvement over soil water content (Fig. 7). Furthermore, the improvement held true regardless of which monthly period was used to represent the 2000–2003 drought (Fig. 7). Among the monthly average soil moisture used to estimate 1D safety loss, June soil water content achieved the highest R^2, whereas August soil water content had the lowest R^2. Moreover, early summer months are most suitable for selecting the initial water content as they represent the water status at the beginning of the pre-monsoon dry period. Consequently, June soil water content was used in the following analysis.

1D vs 3D safety loss as correlates of drought-induced mortality

The explanatory power of 3D safety loss, $\Delta p(\theta_{3D})$, although improved over soil water content, was not consistently higher than that of $\Delta p(\theta_{1D})$ (Fig. 7), suggesting that the influence of lateral convergence was not important across all topographic positions of the landscape. Mortality also exhibited conflicting patterns in relation to putative gradients in lateral flow (Fig. 6). Therefore, we divided the landscape into different topographic categories to find where 1D vs 3D safety loss was the better explanatory factor. Seven categories of topographic positions were defined based on elevation, convergent/divergent ($\delta > 0$ or $\delta < 0$), and hillslope aspects (Table 3).

For convergent and low-elevation areas, 3D safety loss demonstrated clear improvement of R^2 over 1D safety loss, even considering uncertainties associated with m and the reference curves used to derive the metric (Fig. 8). The value of m contributed a ± 0.05 variation in R^2 (Fig. S3). By comparison, 1D safety loss achieved marginally higher explanatory power than 3D safety loss in high elevations, where the explanatory power of 3D safety loss was very sensitive to the value of m and was highest at a low m (Figs 8, S3). However, for mortality in divergent, low-elevation and S–W aspect regions, 3D safety loss had high R^2 but a negative regression slope (Figs 8, S3).

Discussion

Simulations of hydraulic safety loss using TREES

Plants respond to the hydraulic status of both soil and plant xylem, which can only be derived using models that explicitly solve the water transport through the full soil–plant–atmosphere continuum (Sperry *et al.*, 1998; Mackay *et al.*, 2015; Sperry & Love, 2015). The Terrestrial Regional Ecosystem Exchange Simulator (TREES) reasonably captured the variations of sap flux, leaf water potential and, consequently, the whole plant hydraulic conductance over time and across stands (Fig. 4), lending support to using it as a tool to establish the hydraulic safety loss function from a small number of physiological measurements.

Plant hydraulic safety margin, or the difference between E_{crit} and E_c, diminished monotonically with declining soil moisture

Table 3 The sample size (number of groups) and the percentage of total aspen covered areas in the study region for each topographic category

	N–E			S–W			
	Convergent		Divergent	Convergent		Divergent	
Topographic categories	Low	High		Low	High	Low	High
Sample size	32	14	34	31	16	19	15
% of total aspen coverage	16%	6%	29%	13%	6%	10%	19%

Topographic categories were classified according to elevation, aspect and topographic convergence/divergence based on distinctive patterns of mortality shown in Fig. 6.
Low, elevation < 3000 m except for divergent areas on S–W aspect used < 2800 m as low; high, elevation > 3000 m except for divergent areas on S–W aspect used > 2800 as high.
Convergent, $\delta > 0$; Divergent, $\delta < 0$.

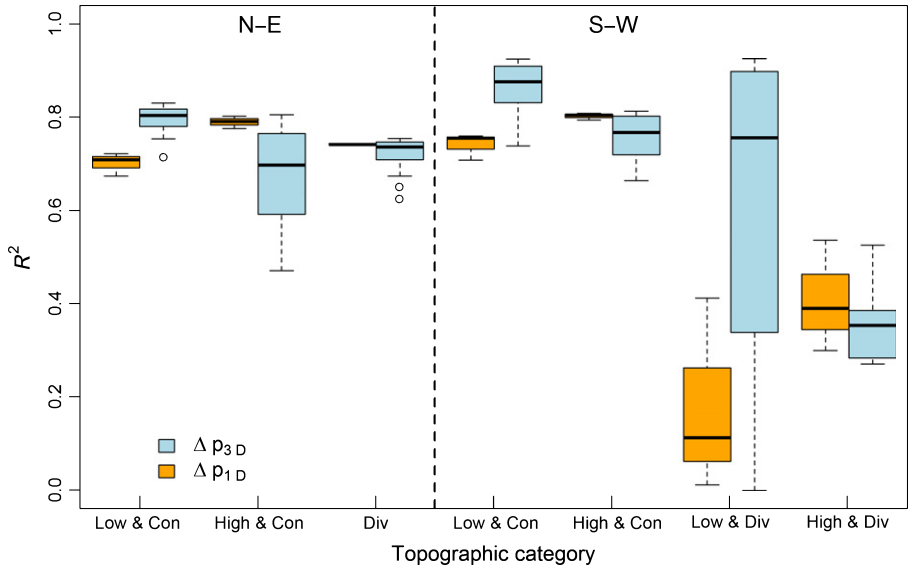

Fig. 8 Box plot showing variance of aspen mortality explained by 3D safety loss and 1D safety loss functions across different topographic positions. Low, elevation < 3000 m (except for the divergent areas on S–W aspect using < 2800 m as low); high, elevation > 3000 m (except for the divergent areas on S–W aspect using > 2800 m as high); convergent (Con), $\delta > 0$; divergent (Div), $\delta < 0$ All three sets of safety loss reference curves (shown in Fig. 4) were used in the calculation of 1D and 3D safety loss; values of *m* used in estimating 3D safety loss ranged from 0.001 to 0.010 with increments of 0.001. Boxplots show the median (bar), interquartile range (box) and outliers (points).

over time, as has been shown in previous studies (Sperry *et al.*, 1998; Hacke *et al.*, 2000)(Fig. 4). The reference curves simulated using TREES reasonably captured the relative differentiation of safety loss due to soil water content and soil types (Fig. 5). The higher safety loss associated with soils with higher clay content was consistent with previous findings of higher plant stress in fine-textured soils compared to coarse-textured soils (Cobb *et al.*, 1997; Sperry & Hacke, 2002; Gitlin *et al.*, 2006).

The reference curves, however, exhibited relatively little sensitivity to the time course of meteorological conditions and the magnitude of vapor pressure deficit (VPD) (Fig. S2). This was likely because the average value of hydraulic safety loss was taken over a sustained period encompassing a wide range of meteorological conditions such as temperature, VPD and solar radiation. The consistent shift of reference curves to higher initial soil water levels, as the rainless period increased from 5 to 7 wk (Fig. S2), highlighted the role of drought duration in addition to intensity in impairing plant function (Dale *et al.*, 2001).

Observed topographic variations in aspen mortality

Mortality severity varied strongly with elevation (Fig. 6), confirming that drought-induced tree mortality was nonrandom over space (Suarez *et al.*, 2004; Gitlin *et al.*, 2006; Kaiser *et al.*, 2013). Changes in aspen mortality severity along elevation gradients shown here were consistent with previous studies of multiple other species in southwestern USA (Allen & Breshears, 1998; Gitlin *et al.*, 2006; Worrall *et al.*, 2008). Mortality severity peaked at lower elevations than the elevation zone with highest aspen abundance (Fig. 6), confirming that aspen in the xeric end of its range within the study area was more susceptible to drought (Frey *et al.*, 2004; Rehfeldt *et al.*, 2009; Michaelian *et al.*, 2011; Worrall *et al.*, 2013).

The secondary control of topographic convergence on forest die-off is less well established in the literature (Bellingham & Tanner, 2000; Worrall *et al.*, 2010; de Toledo *et al.*, 2012). Our results suggested that this may be because topographic convergence affected mortality only in certain parts of the landscape (Figs 6, 8). In other words, trees in valley bottoms were more likely to be impacted by increased water supply due to topographic convergence, whereas trees on hillslope ridges were not. Moreover, unseen subsurface processes, such as interaction between plant roots and bedrock fractures, likely modulated the severity of drought mortality.

Hydraulic safety loss vs soil water content as correlates of drought-induced mortality

We found strong support for our first hypothesis that hydraulic safety loss better explains mortality than soil water content, regardless of uncertainties associated with reference curves used to estimate safety loss (Table 2; Fig. 7). Compared to soil water content, the reference curves incorporated the nonlinear response of safety loss to soil water content and soil texture (Fig. 5). Although the nonlinear response of safety loss to soil water was a better correlate of mortality than soil water content alone ($\Delta p(\theta_{1D})$* vs $\Delta\theta_{1D}$ in Table 2), mortality prediction was further improved when soil type was included ($\Delta p(\theta_{1D})$* vs $\Delta p(\theta_{1D})$ in Table 2). This extended previous findings that both plant xylem and soil were important in predicting plant hydraulic stress (Bréda *et al.*, 2006; Manzoni *et al.*, 2013) to regional scale modeling where it has been largely ignored (Anderegg et al., 2013a; Worrall *et al.*, 2013; but see Anderegg *et al.*, 2015).

We also found improved predictions of mortality when we derived safety loss using early summer months as the initial soil moisture for computing safety loss (Fig. 7). This was likely because plant growth depends heavily on the supply of soil water early in the growing season in southwestern US mountainous environments (Hanson & Weltzin, 2000; Bigler *et al.*, 2007; Williams *et al.*, 2013) and soil was, in general, dry for most locations by August (Fig. S1). Indeed, water stress in May or June has catastrophic impacts on plants, because this is the most active period for plant carbon uptake when high water supply coincides with long daylight hours (Hanson & Weltzin, 2000; Bigler *et al.*,

2007). Moreover, early season drought in the US southwest results in a prolonged growing season water stress, which is important because tree mortality appears to be more closely related to the time spent with extensive stress rather than specific thresholds (McDowell *et al.*, 2013).

1D vs 3D safety loss in relation to drought-induced mortality

Considering our second hypothesis that topographic convergence mediates mortality severity by creating variations of soil water content, we found mixed support. The improvement of 3D safety loss over 1D safety loss to explain mortality was not observed in all topographic situations across the landscape (Figs 7, 8). We did, however, find evidence of improved prediction in low-elevation, topographic convergent regions with relatively less severe mortality (Fig. 8), because of the higher soil water levels, as represented in the 3D mode,l for these areas (Fig. 9b,d,h). The spatial variation of soil moisture remains a challenge to quantify accurately, even using detailed ground-based surveys (Western *et al.*, 1999; Seneviratne *et al.*, 2010; Crow *et al.*, 2012). Nevertheless, given the strong feedbacks between soil moisture and vegetation (Seneviratne *et al.*, 2010), the pattern of vegetation dynamics was indicative of the role played by topographic structure on long-term average soil water content, despite the simple approximation of our 3D model. Our results, along with previous fine-scale studies (Segura *et al.*, 2002; Tromp-van Meerveld & McDonnell, 2006; Adelman *et al.*, 2008; Loranty *et al.*, 2008; Adams *et al.*, 2014), suggest the importance of topographic convergence in mediating plant growth or dieback.

We found contradictory patterns of mortality in convex regions that were neither well captured by 1D nor 3D safety loss (Figs 6, 9a,g). Low-elevation, divergent areas on S–W

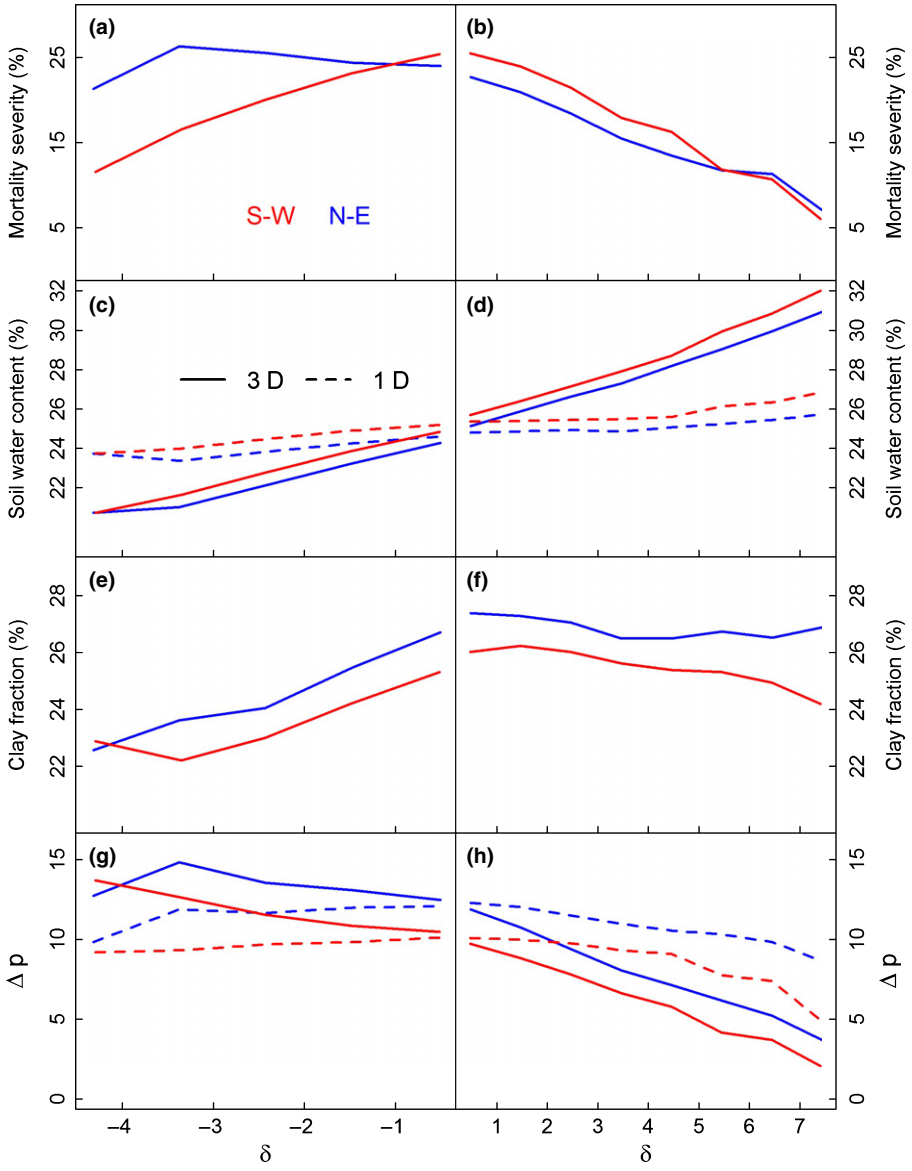

Fig. 9 Mean values of observed mortality rates, soil water content (θ_{1D} and θ_{3D}), soil clay content, absolute and relative vulnerability models along topographic gradient (δ) for divergent regions (a, c, e, g) and convergent regions (b, d, f, h) in low-elevation zones (elevation < 3000 m). Red, S–W hillslope aspect; blue, N–E facing hillslopes. Solid line, 3D estimation of soil water content and safety loss; dashed line, 1D estimation of soil water content and safety loss. 1D safety loss was derived using June soil moisture and the reference curves with 'medium' vulnerability. 3D safety loss was based on $m = 0.007$.

hillslopes were expected to be the driest among all topographic positions, and yet they showed suppressed mortality with more negative δ. This could be attributed to decreased clay content (Fig. 9e), because safety loss was higher for plants in soils with higher clay content (Fig. 5). It could be also related to reduced interspecies competition (Scholes & Archer, 1997) as the more divergent regions tend to be dry and species-poor (Zinko *et al.*, 2005). Given that these very dry locations were likely to be unfavorable for aspen, trees in these areas could have adapted to the low water availability and become more resistant to drought, through altered physiological or morphological traits (Hacke *et al.*, 2000; Joslin *et al.*, 2000; Bréda *et al.*, 2006; Hales *et al.*, 2009). In particular, aspen has been found to have lower vulnerability to cavitation on dry sites compared to wet sites (Anderegg & HilleRisLambers, 2016). Alternatively, plant roots could have obtained water stored in rock fractures (Brooks *et al.*, 2015 and references therein). Although these areas represented 10% of total aspen coverage in this study (Fig. 6d), the survival of some aspen stands under extremely dry conditions suggests that we currently lack the data or model mechanisms required to explain mortality at these locations.

Methodology limitations

We stress that our approach served mainly as a first-order approximation with which to explore the importance of plant hydraulics and lateral groundwater flow for explaining regional-scale mortality. Several caveats can be identified. First, the complex response of plant hydraulics to drought was encapsulated in a single rhizosphere–plant hydraulic continuum exposed to different initial soil water contents and soil textures, and this scheme was upscaled using modeled monthly average soil moisture. Although it was sufficient to demonstrate the utility of plant hydraulics to explain spatial patterns of mortality at the regional extent and monthly time scale, the amplifying effects of rising temperature and repeated drought with sporadic rainfall events were ignored, which could be critical in predicting the timing of a 'mortality crash' for individual trees (Adams *et al.*, 2009; Anderegg *et al.*, 2015). Second, the spatial estimation of safety loss assumed the measured healthy aspen stand to be representative of aspen across the study extent, yet potential variations of physiological traits by genotypic and phenotypic plasticity (e.g. rooting profile and hydraulic vulnerability) could be an important local driver of dieback (Frey *et al.*, 2004; Suarez *et al.*, 2004). Third, we relied on an LSM simulated product to account for the spatial variations of energy and water supply due to elevation and aspect, and used a topography–soil index as a proxy of topographic convergence effects on soil moisture organization. But the complex energy, water and subsurface/soil interactions as well as plant feedbacks were not resolved within an LSM simulated cell, which might be responsible for the limited improvement of our 3D model. Further improvements could be made by incorporating the transient responses of soil moisture to snow distribution and snowmelt, groundwater flow and feedback from plant transpiration (Brooks *et al.*, 2015; Clark *et al.*, 2015).

Implications

This study provided a substantial step beyond previous work by developing a simple, yet realistic hydraulic safety loss function that captured the first-order response of plant hydraulics to climatic water stress and soil water status. Although our model was quite simple, it represented our state-of-knowledge of plant mortality mechanisms. Employing plant hydraulic safety loss greatly improved the ability to explain mortality patterns over soil water content alone, providing support for incorporating physiological mechanisms of tree mortality into Dynamic Global Vegetation Models (DGVMs). Furthermore, our approach can be generalized for multiple species and shows promising scalability from the stand to regional scale.

The physiologically based metric of safety loss served as a useful tool to test hypotheses regarding the spatial controls of drought-induced mortality, which was essential to making predictions over larger areas with limited data (Brooks *et al.*, 2011; Voepel *et al.*, 2011; Adam *et al.*, 2014). Our results provided evidence of topography in mediating tree mortality during drought, especially for convergent topographic areas at low elevation where there was high transpiration demand. These microsite conditions can be critical to understanding species survival/extinction from extended drought under future climate scenarios (Brooks *et al.*, 2015; Clark *et al.*, 2015). Our first-order approximation underscored the relevance of plant hydraulics and topographic processes in understanding forest mortality pattern. Therefore, there is a need for improved models and observations that allow coupling plant hydraulics with spatially distributed microsite conditions to fully understand forest ecosystem response across landscapes of complex topography and its feedbacks to climate change droughts.

Acknowledgements

The data used in this study were acquired as part of the mission of NASA's Earth Science Division, and archived and distributed by the Goddard Earth Sciences (GES) Data and Information Services Center (DISC). Funding for this study was from the National Science Foundation (NSF) through grants IOS 1450679 and IOS 1450650. The views expressed in this manuscript reflect those of the authors and do not necessarily reflect those of the NSF. The authors would like to thank the insightful comments from the Editor and three anonymous reviewers that greatly helped to improve the manuscript.

Author contributions

X.T. and D.S.M. planned and designed the research; X.T. performed research; W.R.L.A. conducted fieldwork; X.T. analysed data; X.T., D.S.M., W.R.L.A., J.S.S. and P.D.B. wrote the manuscript.

References

Adam JC, Stephens JC, Chung SH, Brady MP, Evans RD, Kruger CE, Lamb BK, Liu M, Stöckle CO, Vaughan JK. 2014. BioEarth: envisioning and developing a new regional earth system model to inform natural and agricultural resource management. *Climatic Change* **129**: 555–571.

Adams HR, Barnard HR, Loomis AK. 2014. Topography alters tree growth–climate relationships in a semi-arid forested catchment. *Ecosphere* **5**: art148.

Adams HD, Guardiola-Claramonte M, Barron-Gafford GA, Villegas JC, Breshears DD, Zou CB, Troch PA, Huxman TE. 2009. Temperature sensitivity of drought-induced tree mortality portends increased regional die-off under global-change-type drought. *Proceedings of the National Academy of Sciences, USA* **106**: 7063–7066.

Adelman JD, Ewers BE, MacKay DS. 2008. Use of temporal patterns in vapor pressure deficit to explain spatial autocorrelation dynamics in tree transpiration. *Tree Physiology* **28**: 647–658.

Allen CD, Breshears DD. 1998. Drought-induced shift of a forest–woodland ecotone: rapid landscape response to climate variation. *Proceedings of the National Academy of Sciences, USA* **95**: 14 839–14 842.

Allen CD, Macalady AK, Chenchouni H, Bachelet D, McDowell N, Vennetier M, Kitzberger T, Rigling A, Breshears DD, Hogg E. 2010. A global overview of drought and heat-induced tree mortality reveals emerging climate change risks for forests. *Forest Ecology and Management* **259**: 660–684.

Anderegg LD, Anderegg WR, Abatzoglou J, Hausladen AM, Berry JA. 2013a. Drought characteristics' role in widespread aspen forest mortality across Colorado, USA. *Global Change Biology* **19**: 1526–1537.

Anderegg WR, Anderegg LD, Berry JA, Field CB. 2014. Loss of whole-tree hydraulic conductance during severe drought and multi-year forest die-off. *Oecologia* **175**: 11–23.

Anderegg WR, Berry JA, Smith DD, Sperry JS, Anderegg LD, Field CB. 2012. The roles of hydraulic and carbon stress in a widespread climate-induced forest die-off. *Proceedings of the National Academy of Sciences, USA* **109**: 233–237.

Anderegg WR, Flint A, Huang C-y, Flint L, Berry JA, Davis FW, Sperry JS, Field CB. 2015. Tree mortality predicted from drought-induced vascular damage. *Nature Geoscience* **8**: 367–371.

Anderegg LD, HilleRisLambers J. 2016. Drought stress limits the geographic ranges of two tree species via different physiological mechanisms. *Global Change Biology* **22**: 1029–1045.

Anderegg WR, Kane JM, Anderegg LD. 2013b. Consequences of widespread tree mortality triggered by drought and temperature stress. *Nature Climate Change* **3**: 30–36.

Anderegg WR, Plavcová L, Anderegg LD, Hacke UG, Berry JA, Field CB. 2013c. Drought's legacy: multiyear hydraulic deterioration underlies widespread aspen forest die-off and portends increased future risk. *Global Change Biology* **19**: 1188–1196.

Andreadis KM, Lettenmaier DP. 2006. Trends in 20th century drought over the continental United States. *Geophysical Research Letters* **33**: L10403.

Bartos DL. 2008. *Great Basin aspen ecosystems. Collaborative Management and Research in the Great Basin: examining the issues and developing a framework for action.* Fort Collins, CO, USA: US Department of Agriculture, Forest Service, Rocky Mountain Research Station: General Technical Report RMRS-GTR-204: 57–60.

Bellingham P, Tanner E. 2000. The influence of topography on tree growth, mortality, and recruitment in a tropical montane forest1. *Biotropica* **32**: 378–384.

Beven K, Kirkby M. 1979. A physically based, variable contributing area model of basin hydrology/Un modèle à base physique de zone d'appel variable de l'hydrologie du bassin versant. *Hydrological Sciences Journal* **24**: 43–69.

Bigler C, Gavin DG, Gunning C, Veblen TT. 2007. Drought induces lagged tree mortality in a subalpine forest in the Rocky Mountains. *Oikos* **116**: 1983–1994.

Bréda N, Huc R, Granier A, Dreyer E. 2006. Temperate forest trees and stands under severe drought: a review of ecophysiological responses, adaptation processes and long-term consequences. *Annals of Forest Science* **63**: 625–644.

Breshears DD, Myers OB, Meyer CW, Barnes FJ, Zou CB, Allen CD, McDowell NG, Pockman WT. 2008. Tree die-off in response to global change-type drought: mortality insights from a decade of plant water potential measurements. *Frontiers in Ecology and the Environment* **7**: 185–189.

Brooks PD, Chorover J, Fan Y, Godsey SE, Maxwell RM, McNamara JP, Tague C. 2015. Hydrological partitioning in the critical zone: recent advances and opportunities for developing transferable understanding of water cycle dynamics. *Water Resources Research* **51**: 6973–6987.

Brooks PD, Troch PA, Durcik M, Gallo E, Schlegel M. 2011. Quantifying regional scale ecosystem response to changes in precipitation: not all rain is created equal. *Water Resources Research* **47**: W00J08.

Chen J, Kumar P. 2001. Topographic influence on the seasonal and interannual variation of water and energy balance of basins in North America. *Journal of Climate* **14**: 1989–2014.

Clark MP, Fan Y, Lawrence DM, Adam JC, Bolster D, Gochis DJ, Hooper RP, Kumar M, Leung LR, Mackay DS. 2015. Improving the representation of hydrologic processes in Earth System Models. *Water Resources Research* **51**: 5929–5956.

Cobb NS, Mopper S, Gehring CA, Caouette M, Christensen KM, Whitham TG. 1997. Increased moth herbivory associated with environmental stress of pinyon pine at local and regional levels. *Oecologia* **109**: 389–397.

Crow WT, Berg AA, Cosh MH, Loew A, Mohanty BP, Panciera R, Rosnay P, Ryu D, Walker JP. 2012. Upscaling sparse ground-based soil moisture observations for the validation of coarse-resolution satellite soil moisture products. *Reviews of Geophysics* **50**: RG2002.

Dale VH, Joyce LA, McNulty S, Neilson RP, Ayres MP, Flannigan MD, Hanson PJ, Irland LC, Lugo AE, Peterson CJ. 2001. Climate change and forest disturbances climate change can affect forests by altering the frequency, intensity, duration, and timing of fire, drought, introduced species, insect and pathogen outbreaks, hurricanes, windstorms, ice storms, or landslides. *BioScience* **51**: 723–734.

Danielson JJ, Gesch DB. 2011. *Global multi-resolution terrain elevation data 2010 (GMTED2010).* Reston, VA, USA: US Geological Survey.

Dawson TE. 1993. Hydraulic lift and water use by plants: implications for water balance, performance and plant-plant interactions. *Oecologia* **95**: 565–574.

Dingman LS. 1994. *Physical hydrology.* New York, NY, USA: Macmillan.

Famiglietti J, Wood E. 1994. Multiscale modeling of spatially variable water and energy balance processes. *Water Resources Research* **30**: 3061–3078.

Fan Y. 2015. Groundwater in the Earth's critical zone – relevance to large-scale patterns and processes. *Water Resources Research* **51**: 3052–3069.

Fisher R, McDowell N, Purves D, Moorcroft P, Sitch S, Cox P, Huntingford C, Meir P, Ian Woodward F. 2010. Assessing uncertainties in a second-generation dynamic vegetation model caused by ecological scale limitations. *New Phytologist* **187**: 666–681.

Franklin JF, Shugart H, Harmon ME. 1987. Tree death as an ecological process. *BioScience* **37**: 550–556.

Frey BR, Lieffers VJ, Hogg E, Landhäusser SM. 2004. Predicting landscape patterns of aspen dieback: mechanisms and knowledge gaps. *Canadian Journal of Forest Research* **34**: 1379–1390.

Friend AD, Lucht W, Rademacher TT, Keribin R, Betts R, Cadule P, Ciais P, Clark DB, Dankers R, Falloon PD. 2014. Carbon residence time dominates uncertainty in terrestrial vegetation responses to future climate and atmospheric CO_2. *Proceedings of the National Academy of Sciences, USA* **111**: 3280–3285.

Fritts HC. 1974. Relationships of ring widths in arid-site conifers to variations in monthly temperature and precipitation. *Ecological Monographs* **44**: 411–440.

Gaylord ML, Kolb TE, Pockman WT, Plaut JA, Yepez EA, Macalady AK, Pangle RE, McDowell NG. 2013. Drought predisposes piñon–juniper woodlands to insect attacks and mortality. *New Phytologist* **198**: 567–578.

Gitlin AR, Sthultz CM, Bowker MA, Stumpf S, Paxton KL, Kennedy K, Muñoz A, Bailey JK, Whitham TG. 2006. Mortality gradients within and among dominant plant populations as barometers of ecosystem change during extreme drought. *Conservation Biology* **20**: 1477–1486.

Granier A, Loustau D. 1994. Measuring and modelling the transpiration of a maritime pine canopy from sap-flow data. *Agricultural and Forest Meteorology* **71**: 61–81.

GRASS Development Team. 2014. *Geographic resources analysis support system (GRASS) software, version 6.4.* Open Source Geospatial Foundation. http://grass.osgeo.org.

Hacke U, Sperry J, Ewers B, Ellsworth D, Schäfer K, Oren R. 2000. Influence of soil porosity on water use in *Pinus taeda*. *Oecologia* **124**: 495–505.

Hales T, Ford C, Hwang T, Vose J, Band L. 2009. Topographic and ecologic controls on root reinforcement. *Journal of Geophysical Research: Earth Surface (2003–2012)* **114**(F3): F03013.

Hanson PJ, Weltzin JF. 2000. Drought disturbance from climate change: response of United States forests. *Science of the Total Environment* **262**: 205–220.

Hartmann H, Adams HD, Anderegg WR, Jansen S, Zeppel MJ. 2015. Research frontiers in drought-induced tree mortality: crossing scales and disciplines. *New Phytologist* **205**: 965–969.

Hogg E, Brandt J, Michaelian M. 2008. Impacts of a regional drought on the productivity, dieback, and biomass of western Canadian aspen forests. *Canadian Journal of Forest Research* **38**: 1373–1384.

Huang CY, Anderegg WR. 2012. Large drought-induced aboveground live biomass losses in southern Rocky Mountain aspen forests. *Global Change Biology* **18**: 1016–1027.

Joslin J, Wolfe M, Hanson P. 2000. Effects of altered water regimes on forest root systems. *New Phytologist* **147**: 117–129.

Kaiser KE, McGlynn BL, Emanuel RE. 2013. Ecohydrology of an outbreak: mountain pine beetle impacts trees in drier landscape positions first. *Ecohydrology* **6**: 444–454.

Körner C. 2007. The use of 'altitude' in ecological research. *Trends in Ecology & Evolution* **22**: 569–574.

Lammers RB, Band LE. 1990. Automating object representation of drainage basins. *Computers & Geosciences* **16**: 787–810.

Liu Y, Pereira L, Fernando R. 2006. Fluxes through the bottom boundary of the root zone in silty soils: parametric approaches to estimate groundwater contribution and percolation. *Agricultural Water Management* **84**: 27–40.

Loranty MM, Mackay DS, Ewers BE, Adelman JD, Kruger EL. 2008. Environmental drivers of spatial variation in whole-tree transpiration in an aspen-dominated upland-to-wetland forest gradient. *Water Resources Research* **44**: W02441.

Lowry J, Ramsey R, Thomas K, Schrupp D, Sajwaj T, Kirby J, Waller E, Schrader S, Falzarano S, Langs L. 2007. Mapping moderate-scale land-cover over very large geographic areas within a collaborative framework: a case study of the Southwest Regional Gap Analysis Project (SWReGAP). *Remote Sensing of Environment* **108**: 59–73.

Mackay DS, Roberts DE, Ewers BE, Sperry JS, McDowell NG, Pockman WT. 2015. Interdependence of chronic hydraulic dysfunction and canopy processes can improve integrated models of tree response to drought. *Water Resources Research* **51**: 6156–6176.

Manzoni S, Vico G, Porporato A, Katul G. 2013. Biological constraints on water transport in the soil–plant–atmosphere system. *Advances in Water Resources* **51**: 292–304.

McDonnell J, Sivapalan M, Vaché K, Dunn S, Grant G, Haggerty R, Hinz C, Hooper R, Kirchner J, Roderick M. 2007. Moving beyond heterogeneity and process complexity: a new vision for watershed hydrology. *Water Resources Research* **43**: W07301.

McDowell NG, Beerling DJ, Breshears DD, Fisher RA, Raffa KF, Stitt M. 2011. The interdependence of mechanisms underlying climate-driven vegetation mortality. *Trends in Ecology & Evolution* **26**: 523–532.

McDowell NG, Fisher RA, Xu C, Domec J, Hölttä T, Mackay DS, Sperry JS, Boutz A, Dickman L, Gehres N. 2013. Evaluating theories of drought-induced vegetation mortality using a multimodel–experiment framework. *New Phytologist* **200**: 304–321.

McDowell N, Pockman WT, Allen CD, Breshears DD, Cobb N, Kolb T, Plaut J, Sperry J, West A, Williams DG. 2008. Mechanisms of plant survival and mortality during drought: why do some plants survive while others succumb to drought? *New Phytologist* **178**: 719–739.

Mencuccini M. 2003. The ecological significance of long-distance water transport: short-term regulation, long-term acclimation and the hydraulic costs of stature across plant life forms. *Plant, Cell & Environment* **26**: 163–182.

Michaelian M, Hogg EH, Hall RJ, Arsenault E. 2011. Massive mortality of aspen following severe drought along the southern edge of the Canadian boreal forest. *Global Change Biology* **17**: 2084–2094.

Moore ID, Gessler P, Nielsen G, Peterson G. 1993. Soil attribute prediction using terrain analysis. *Soil Science Society of America Journal* **57**: 443–452.

Nijssen B, Schnur R, Lettenmaier DP. 2001. Global retrospective estimation of soil moisture using the variable infiltration capacity land surface model, 1980–93. *Journal of Climate* **14**: 1790–1808.

Niu GY, Yang ZL, Dickinson RE, Gulden LE. 2005. A simple TOPMODEL-based runoff parameterization (SIMTOP) for use in global climate models. *Journal of Geophysical Research: Atmospheres (1984–2012)* **110**: D21.

Oglesby RJ. 1991. Springtime soil moisture, natural climatic variability, and North American drought as simulated by the NCAR Community Climate Model 1. *Journal of Climate* **4**: 890–897.

Powell TL, Galbraith DR, Christoffersen BO, Harper A, Imbuzeiro H, Rowland L, Almeida S, Brando PM, Costa ACL, Costa MH. 2013. Confronting model predictions of carbon fluxes with measurements of Amazon forests subjected to experimental drought. *New Phytologist* **200**: 350–365.

Quinn P, Beven K, Lamb R. 1995. The in (a/tan/β) index: how to calculate it and how to use it within the topmodel framework. *Hydrological Processes* **9**: 161–182.

R Core Team. 2015. *R: a language and environment for statistical computing.* [WWW document] URL https://www.R-project.org/ Vienna, Austria: R Foundation for Statistical Computing.

Rehfeldt GE, Ferguson DE, Crookston NL. 2009. Aspen, climate, and sudden decline in western USA. *Forest Ecology and Management* **258**: 2353–2364.

Rinehart AJ, Vivoni ER, Brooks PD. 2008. Effects of vegetation, albedo, and solar radiation sheltering on the distribution of snow in the Valles Caldera, New Mexico. *Ecohydrology* **1**: 253–270.

Robock A, Luo L, Wood EF, Wen F, Mitchell KE, Houser PR, Schaake JC, Lohmann D, Cosgrove B, Sheffield J. 2003. Evaluation of the North American Land Data Assimilation System over the southern Great Plains during the warm season. *Journal of Geophysical Research: Atmospheres (1984–2012)* **108**(D22): 8846.

Scholes R, Archer S. 1997. Tree-grass interactions in savannas. *Annual review of Ecology and Systematics* **28**: 517–544.

Segura G, Balvanera P, Durán E, Pérez A. 2002. Tree community structure and stem mortality along a water availability gradient in a Mexican tropical dry forest. *Plant Ecology* **169**: 259–271.

Seneviratne SI, Corti T, Davin EL, Hirschi M, Jaeger EB, Lehner I, Orlowsky B, Teuling AJ. 2010. Investigating soil moisture–climate interactions in a changing climate: a review. *Earth-Science Reviews* **99**: 125–161.

Sheffield J, Goteti G, Wen F, Wood EF. 2004. A simulated soil moisture based drought analysis for the United States. *Journal of Geophysical Research: Atmospheres (1984–2012)* **109**(D24): D24108.

Sheffield J, Wood EF. 2008. Global trends and variability in soil moisture and drought characteristics, 1950–2000, from observation-driven simulations of the terrestrial hydrologic cycle. *Journal of Climate* **21**: 432–458.

Sivapalan M, Beven K, Wood EF. 1987. On hydrologic similarity: 2. A scaled model of storm runoff production. *Water Resources Research* **23**: 2266–2278.

Sperry J, Adler F, Campbell G, Comstock J. 1998. Limitation of plant water use by rhizosphere and xylem conductance: results from a model. *Plant, Cell & Environment* **21**: 347–359.

Sperry J, Hacke U. 2002. Desert shrub water relations with respect to soil characteristics and plant functional type. *Functional Ecology* **16**: 367–378.

Sperry JS, Love DM. 2015. What plant hydraulics can tell us about responses to climate-change droughts. *New Phytologist* **207**: 14–27.

Suarez ML, Ghermandi L, Kitzberger T. 2004. Factors predisposing episodic drought-induced tree mortality in *Nothofagus*–site, climatic sensitivity and growth trends. *Journal of Ecology* **92**: 954–966.

Thompson SE, Harman CJ, Troch PA, Brooks PD, Sivapalan M. 2011. Spatial scale dependence of ecohydrologically mediated water balance partitioning: a synthesis framework for catchment ecohydrology. *Water Resources Research* **47**: W00J03.

de Toledo JJ, Magnusson WE, Castilho CV, Nascimento HE. 2012. Tree mode of death in Central Amazonia: effects of soil and topography on tree mortality associated with storm disturbances. *Forest Ecology and Management* **263**: 253–261.

Tromp-van Meerveld H, McDonnell J. 2006. On the interrelations between topography, soil depth, soil moisture, transpiration rates and species distribution at the hillslope scale. *Advances in Water Resources* **29**: 293–310.

USDA NRCS. 2014. *U.S. general soil map (STATSGO2) by state.* Washington, DC, USA: Natural Resources Conservation Service USDA.

Voepel H, Ruddell B, Schumer R, Troch PA, Brooks PD, Neal A, Durcik M, Sivapalan M. 2011. Quantifying the role of climate and landscape characteristics on hydrologic partitioning and vegetation response. *Water Resources Research* **47**: W00J09.

Waring RH. 1987. Characteristics of trees predisposed to die. *BioScience* **37**: 569–574.

Western AW, Grayson RB, Blöschl G, Willgoose GR, McMahon TA. 1999. Observed spatial organization of soil moisture and its relation to terrain indices. *Water Resources Research* **35**: 797–810.

Williams AP, Allen CD, Macalady AK, Griffin D, Woodhouse CA, Meko DM, Swetnam TW, Rauscher SA, Seager R, Grissino-Mayer HD. 2013. Temperature as a potent driver of regional forest drought stress and tree mortality. *Nature Climate Change* **3**: 292–297.

Winstral A, Marks D. 2002. Simulating wind fields and snow redistribution using terrain-based parameters to model snow accumulation and melt over a semi-arid mountain catchment. *Hydrological Processes* **16**: 3585–3603.

Wolock DM, Price CV. 1994. Effects of digital elevation model map scale and data resolution. *Water Resources Research* **30**: 3041–3052.

Worrall JJ, Egeland L, Eager T, Mask RA, Johnson EW, Kemp PA, Shepperd WD. 2008. Rapid mortality of *Populus tremuloides* in southwestern Colorado, USA. *Forest Ecology and Management* **255**: 686–696.

Worrall JJ, Marchetti SB, Egeland L, Mask RA, Eager T, Howell B. 2010. Effects and etiology of sudden aspen decline in southwestern Colorado, USA. *Forest Ecology and Management* **260**: 638–648.

Worrall JJ, Rehfeldt GE, Hamann A, Hogg EH, Marchetti SB, Michaelian M, Gray LK. 2013. Recent declines of *Populus tremuloides* in North America linked to climate. *Forest Ecology and Management* **299**: 35–51.

Xia Y, Mitchell K, Ek M, Cosgrove B, Sheffield J, Luo L, Alonge C, Wei H, Meng J, Livneh B. 2012a. Continental-scale water and energy flux analysis and validation for North American Land Data Assimilation System project phase 2 (NLDAS-2): 2. Validation of model-simulated streamflow. *Journal of Geophysical Research: Atmospheres (1984–2012)* **117**: D03110.

Xia Y, Mitchell K, Ek M, Sheffield J, Cosgrove B, Wood E, Luo L, Alonge C, Wei H, Meng J. 2012b. Continental-scale water and energy flux analysis and validation for the North American Land Data Assimilation System project phase 2 (NLDAS-2): 1. Intercomparison and application of model products. *Journal of Geophysical Research: Atmospheres (1984–2012)* **117**: D03109.

Zapata-Rios X, Brooks PD, Troch PA, McIntosh J, Guo Q. 2015. Influence of terrain aspect on water partitioning, vegetation structure and vegetation greening in high-elevation catchments in northern New Mexico. *Ecohydrology*. doi: 10.1002/eco.1674.

Zinko U, Seibert J, Dynesius M, Nilsson C. 2005. Plant species numbers predicted by a topography-based groundwater flow index. *Ecosystems* **8**: 430–441.

Supporting Information

Additional Supporting Information may be found online in the Supporting Information tab for this article:

Fig. S1 Monotonic decline of soil moisture during the growing season from May to August for the 2000–2003 drought and for the 1979–2009 period across Colorado's aspen forest based on variable infiltration capacity (VIC) simulated soil water content.

Fig. S2 Simulations used to generate the ensemble of reference curves in the sensitivity analysis.

Fig. S3 Sensitivity analysis with respect to values of m and the corresponding explanatory power and regression slope of Δp (θ_{3D}) in different topographic areas.

Notes S1 Key processes and parameterizations of TREES.

Please note: Wiley Blackwell are not responsible for the content or functionality of any supporting information supplied by the authors. Any queries (other than missing material) should be directed to the *New Phytologist* Central Office.